

Easily-manufactured paper-based materials with high porosity for adsorption/separation applications in complex wastewater

Shan Jiang¹, Jianfeng Xi¹, Hongqi Dai¹, Huining Xiao (✉)², Weibing Wu (✉)¹

¹ Jiangsu Co-Innovation Center for Efficient Processing and Utilization of Forest Resources, International Innovation Center for Forest Chemicals and Materials, Nanjing Forestry University, Nanjing 210037, China

² Department of Chemical Engineering, University of New Brunswick, Fredericton E3B 5A3, Canada

© Higher Education Press 2023

Abstract A multi-functional porous paper-based material was prepared from grass pulp by simple pore-forming and green cross-linking method. As a pore-forming agent, calcium citrate increased the porosity of the paper-based material from 30% to 69% while retaining the mechanical strength. The covalent cross-linking of citric acid between cellulose fibers improved both the wet strength and adsorption capacity. In addition, owing to the introduction of high-content carboxyl groups as well as the construction of hierarchical micro-nano structure, the underwater oil contact angle was up to 165°. The separation efficiency of the emulsified oil was 99.3%, and the water flux was up to 2020 L·m⁻²·h⁻¹. The theoretical maximum adsorption capacities of cadmium ion, lead ion and methylene blue reached 136, 229 and 128.9 mg·g⁻¹, respectively. The continuous purification of complex wastewater can be achieved by using paper-based materials combined with filtration technology. This work provides a simple, low cost and environmental approach for the treatment of complex wastewater containing insoluble oil, organic dyes, and heavy metal ions.

Keywords adsorption, oil–water separation, underwater superoleophobicity, wastewater treatment

1 Introduction

Freshwater is one of the resources on which all life depends. However, with the development of society and the improvement of people's living standards, various industrial, agricultural and living activities of human

beings have caused an increasingly serious problem of water pollution, which has aroused considerable concern [1]. Water pollution has become one of the most urgent problems to be solved [2]. The wastewater from tanneries, dye plants, oil and gas industries, thermal power facilities and other industries often contains more than one pollutant, resulting in a complex wastewater system that contains emulsified oils, heavy metal ions, dyes and so on [3–5]. Oil pollution in water is concentrated on the water surface, which usually bring catastrophic impacts to the growth of water organisms and even the ecological environment of water [6,7]. Heavy metal ion pollution has posed a serious threat to human health due to the carcinogenicity, enrichment, high toxicity and difficulty in degradation of metal ions [8]. Dye is another nasty pollution in water and the remediation cost is usually high [9]. At present, there are a large number of reports on the treatment of the above three pollutants.

Many approaches have been reported to remove oil or emulsified oil in water, such as adsorption, membrane filtration, centrifugation, electrolysis, chemical flocculation, and chemical dispersion [10,11]. Among them, the filtration membrane materials with underwater superoleophobic properties have become a research hotspot in the field of oil–water separation due to their advantages including oil-contamination resistance, good flexibility, and reusability [12]. The polyvinylidene fluoride and polytetrafluoroethylene with superhydrophilic and underwater superoleophobic properties were prepared by using tannic acid and edible ovalbumin, which had high oil–water mixture separation efficiency, stability and anti-fouling properties [13]. Chen et al. [14] used a vapor–liquid sol–gel process to deposit silica particles with thiols onto cotton fabric, which was further grafted 2-(dimethylamino) ethyl methacrylate via a thiol-ene

click reaction. Because the fabric showed an underwater contact angle of 162° , it can be used for separation of various oil–water mixtures, oil-in-water and water-in-oil emulsions with high separation efficiency. Copper mesh has also been used as the substrates for oil–water separation after the deposition of inorganic sodium silicate and aluminum oxide powders via a layer-by-layer self-assembly process [15].

Various ways have also been used to remove soluble dyes and heavy metal ions, such as chemical precipitation, membrane separation, ion exchange, biological method, and adsorption [16]. Among them, adsorption method has become one of the most widely used methods due to its low cost, simple operation, high reliability and efficiency [17,18]. Liu et al. [19] prepared straw adsorbent with high adsorption capacity by grafting acrylamide and citric acid (CA) for simultaneous adsorption of anionic and cationic pollutants. The graphene oxide-chitosan hydrogels, which were prepared via the self-assembly of graphene oxide sheets and chitosan chains, also showed high adsorption capacity for many contaminants, such as cationic and anionic dyes and metal ions [20]. However, most of the above wastewater treatment methods focus on the removal of single pollutant, making the whole process be cumbersome and inefficient. Therefore, it is particularly important to explore wastewater treatment materials and technology that can simultaneously remove multiple pollutants. Up to now, there are few reports about the preparation of composite materials with both adsorption and separation functions and their applications in the treatment of complex wastewater [21,22]. Moreover, most of the reported composite materials have the problems of complex preparation process, usage of toxic and harmful reagents, or high cost [23–25].

Cellulose fiber has the advantages of extensive sources, low cost, environmental friendliness and easy modification. Paper-based functional materials prepared from cellulose fiber have attracted great attention in water treatment field [26,27]. The paper structural characteristics could improve the practical application performance of membrane separation technology in wastewater treatment and facilitate paper recovery and recycling [28,29]. There are many raw materials that can be used to prepare paper-based functional materials, such as poplar pulp, softwood pulp, wheat straw pulp [30]. Among them, wheat straw pulp has the advantages of lower cost, larger specific surface area, higher lignin content, and richer surface functional groups, which make it good substrate for multicomponent adsorption [31]. However, there are still some shortcomings of paper-based materials made from straw pulp, such as low strength, low porosity, and poor water flux. Therefore, improving the wet strength and porosity is of great significance for the construction of straw-pulp-based functional papers for adsorption/separation application.

In this work, a multifunctional paper-based material with heavy metal ion/dye adsorption and oil–water separation performance was obtained using wheat straw pulp as raw material by simple green cross-linking and pore-forming methods. CA was used as a cross-linking and functional agent to simultaneously increase the wet tensile index and carboxyl content of materials by esterification reaction with cellulose. Calcium citrate (CC), as a pore-making agent, can not only form pores but also further improve the cross-linking between fibers through the CA generated by HCl treatment. In addition, the underwater superoleophobic property was optimized by controlling the surface hydrophilicity and micro-nano structure of paper. The adsorption and separation performances of metal ions, dyes, and emulsified oils for complex wastewater were thoroughly investigated.

2 Experimental

2.1 Materials and reagents

High-yield straw pulp (was provided by Asia Symbol Pulp and Paper Co., Ltd., China). CA, CC, sodium hypophosphite (SHP), methylene blue (MB), oil red (dye content $\geq 75\%$), *n*-hexane, petroleum ether (Sigma-Aldrich). Soybean oil was purchased from Yihai Kerry Food Marketing Co., Ltd. All reagents were analytical grade and require no further purification.

2.2 Preparation of paper-based material

The contents of lignin, cellulose and hemicellulose in wheat straw pulp were 24%, 53% and 18%, respectively. According to Technical Association of the Pulp and Paper Industry (TAPPI) standard of T272, paper sheets with CC (30 wt % of the total dry pulp weight) as filler were prepared. Specific steps are described in the Electronic Supplementary Material (ESM).

The CA solution with the concentration of 8 wt % (CA:SHP with a molar ratio of 2:1) was first prepared. To ensure that the solution was fully absorbed, immersed the paper in the mixed solution until the paper sheets weighs twice as much as the original paper (permissible error $\pm 5\%$). Subsequently, the paper sheets were placed under 160°C for 10 min [32].

2.3 Pore formation of paper-based material

The modified paper was soaked in an excess of $0.1\text{ mol}\cdot\text{L}^{-1}$ HCl solution to ensure complete dissolution of CC in the paper. After 24 h, the paper sample was taken out and washed with deionized water until neutral. Finally, the paper sheets were dried and placed in an environment of temperature 23°C , humidity 50%. The basic naming rules are as follows: Base paper (no CC

added), CBP (CC added), CBPM (CBP modified by CA), Pro-CBPM (CBPM after the removal of CC).

2.4 Oil–water separation

For the oil-in-water emulsions, tween 80 as the emulsifier was dissolved in different oil/water mixtures (petroleum ether, *n*-hexane, and soybean oil) with the volume ratio of 1:100, and then the stable oil-in-water emulsions were obtained by stirring the mixture at 5000 r·min⁻¹ for 5 min.

For the separation process, the paper sheets pre-moistened with water was tightly fixed between two glass tubes, and 300 mL of the mixture was passed only driven under the gravity. The water flux can be characterized via the following Eq. (1):

$$\text{Flux} = V/(S \times t), \quad (1)$$

where S (m²) stands for the effective area of mixture through the paper, V (L) is the volume of the filtrate, and t (h) is the filtration time [33]. The calculation formula of separation efficiency was as follows:

$$\eta = \left(1 - \frac{c_1}{c_0}\right) \times 100\%, \quad (2)$$

where c_0 (mg·mL⁻¹) and c_1 (mg·mL⁻¹) belong to the oil concentrations in the emulsion before and after filtration, respectively.

2.5 Heavy metal ion and dye adsorption

The adsorption experiments were performed by putting 0.4 g Pro-CBPM in a series of flasks containing 200 mL solution of metal ions or dyes with certain concentrations. The flasks were sealed and shook in a rotary shaker (SHA-C, China) with constant rate of 150 r·min⁻¹ at 30 °C for 4 h.

Adsorption experiments were carried out with 200 mg·L⁻¹ Pb(II) and Cd(II) (at pH 5) and 20 mg·L⁻¹ MB solution (at pH 6). Samples were taken within 240 min at regular intervals, and the filtrate was further determined.

For the adsorption isotherms experiments, Pb(II) and Cd(II) solutions of 25, 50, 100, 150, and 200 mg·L⁻¹ were prepared and the pH was adjusted to 5. Similarly, a series of 10, 20, 50, 75, 100 mg·L⁻¹ MB solutions at pH 6 were prepared. The concentration of the residual dye and metal ions solution was analyzed using ultraviolet–visible spectroscopy and inductively coupled plasma spectrometer analysis.

2.6 Measurement of mechanical strength and detection of carboxyl content

The mechanical strength of paper sheets was measured according to the TAPPI standard T494 om-01 and T456 om-03. The details are provided in ESM.

The carboxyl content of Pro-CBPM was determined via conductometric titration. The carboxyl content [C_{COOH} (mmol·g⁻¹)] was calculated as follows:

$$C_{\text{COOH}} = \frac{C_{\text{NaOH}} \times (V_2 - V_1)}{m} \times 1000, \quad (3)$$

where C_{NaOH} is the concentration of NaOH (mol·L⁻¹), V_2 and V_1 are the volumes of NaOH at the beginning and the end of the process (L), m (g) is the quality of the Pro-CBPM [34,35].

The details of characterization are introduced in the ESM.

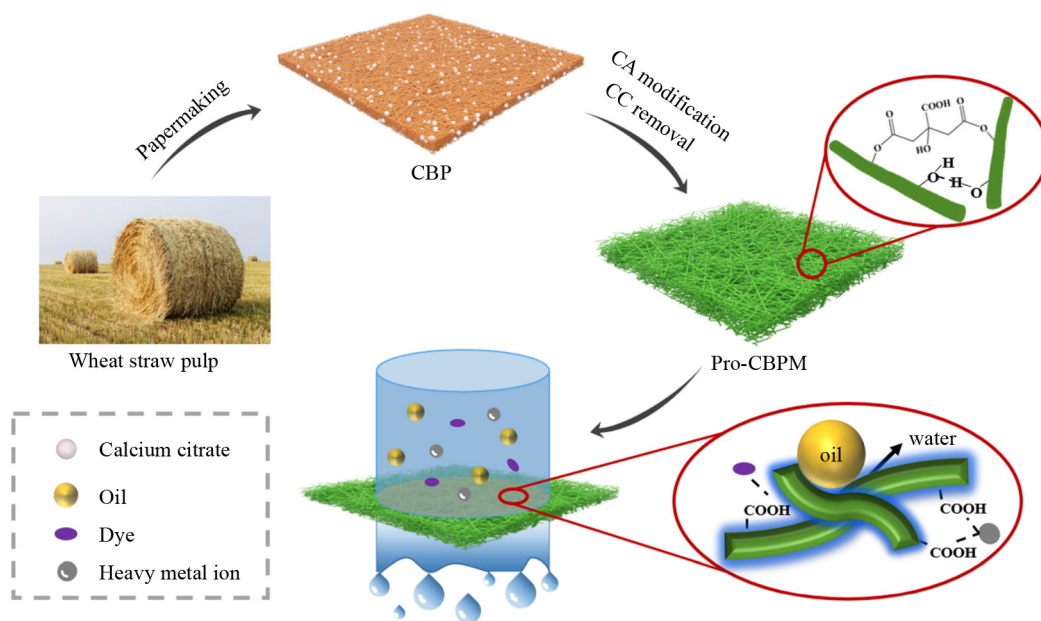
3 Results and discussion

3.1 Fabrication of paper-based multifunctional materials

Scheme 1 shows the synthetic route of paper-based multifunctional materials. Cellulose and residual lignin, as the main component of wheat straw pulp, can be chemically modified by grafting or crosslinking reaction to enhance its binding ability with metal ions and dyes. It is well known that the adsorption properties of materials depend on the number of active functional groups and the specific surface area, and the high porosity has a positive effect on the adsorption capacity. Based on this, CC porogen with the average size of 30 μm, which can be simply removed by the reaction with HCl, is added as filler to produce pores during the papermaking process. Moreover, the reaction of CC with HCl will produce the crosslinker of CA. Esterification between CA and hydroxyl groups on lignocellulose occurs to form a three-dimensional network between fibers. High porosity is not only conducive to the diffusion and adsorption inside the paper-based material, but also improves the water flux and further the processing capacity during the oil–water separation [35]. On the other hand, the process of CA modification is able to introduce a large number of carboxyl functional groups, which endows the material with high adsorption capacity and surface hydrophilicity.

The surface morphologies of the various samples are shown in Fig. 1. The fibers are closely bonded with low porosity, resulting in high fiber compactness and relatively smooth surface. After pore formation, the pores per unit area and the pore size of the Pro-CBPM sample are significantly increased. The rough structure of concave and convex formed on paper is important for the construction of underwater superoleophobic surface. According to the transition state model theory, the increased roughness can change the surface characteristics and lead to the enhancement of wetting property [36]. Because there are lots of hydrophilic groups on the surface of the fiber, the underwater superoleophobicity is improved with the increase of the surface roughness.

Figure S1 (cf. ESM) shows the Fourier transform



Scheme 1 The synthetic route of paper-based multifunctional materials.

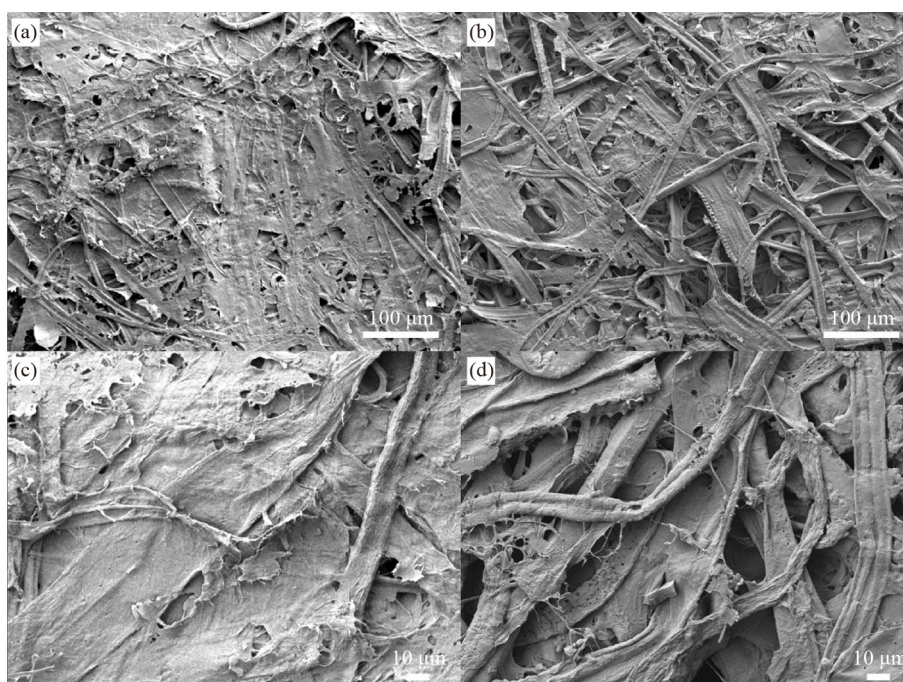


Fig. 1 SEM images of (a) base paper, (b) Pro-CBPM; Magnified SEM images of (c) base paper, (d) Pro-CBPM.

infrared spectra of different papers. The typical characteristic peaks at 3340 and 2900 cm^{-1} correspond to the stretching vibration of $-\text{OH}$ and the $\text{C}-\text{H}$, respectively. Compared with the CBP, the appearance of carboxylic acid group peak at 1723 cm^{-1} in CBPM and Pro-CBPM suggests the successful crosslinking reaction via CA [37]. The surface chemical compositions of different paper samples were evaluated by X-ray photoelectron spectroscopy (Fig. S2, cf. ESM). For the base paper and CBP, there are three peaks at 284.7 , 286.5 , and 288 eV belonging to $\text{C}-\text{C}$, $\text{C}-\text{O}-\text{H}$ and $\text{O}-\text{C}-\text{O}$, respectively. In

the high-resolution $\text{C } 1\text{s}$ spectra of Pro-CBPM (Fig. S2(d)), a new peak at 289 eV associated with $\text{O}=\text{C}-\text{O}$ appears, indicating successful crosslinking between CA and fibers as well as the introduction of carboxyl groups.

3.2 Tensile strength

Figure 2 shows the mechanical strength properties of paper-based materials. Due to short length of straw pulp fiber and poor interfiber binding, the dry and wet tensile strength of the base paper are relatively low. The addition

of fillers further leads to a reduction in the contact area between fibers. The dry strength of paper, which is mainly dependent on the hydrogen bonding, decrease significantly [38]. Similarly, the wet strength of CBP drops from 1.9 to 1.0 $\text{Nm}\cdot\text{g}^{-1}$. After crosslinking with CA, the tensile indexes of CBP are significantly improved. Especially, the wet tensile index is increased by nearly ten times. This can be interpreted that although most of the hydrogen bonding will be broken when the paper is moistened with water, the covalent network formed through cross-linking still maintains the bonding between the fibers.

3.3 Wettability

To verify the underwater wettability of Pro-CBPM, the underwater oil contact angle (UOCA) for different oils and in different pH environments were measured at room temperature, as presented in Fig. 3. The UOCA of CBPM can reach about 150° , which is greatly improved compared with CBP, and the paper sample after pore

formation is further increased to more than 160° , realizing underwater superoleophobicity (Fig. 3(a)). Due to the introduction of a large number of carboxyl groups ($0.91 \text{ mmol}\cdot\text{g}^{-1}$) in the reaction between CA and cellulose, the UOCA of CBPM is up to 150° . According to the principle of surface wettability, hydrophilicity and hierarchical micro-nano structure are the keys to achieve the underwater superhydrophobicity. The pore-forming process not only improves the porosity, but also constructs a rough structure on the material surface [39–41]. Therefore, the UOCA of the Pro-CBPM is further improved to higher than 150° , showing underwater superhydrophobicity.

The wettability stability of modified membrane in harsh environmental conditions (acid and alkali solutions) is another essential factor in practical application [42]. The UOCA of the Pro-CBPM was measured in solutions with different pH values (Fig. 3(b)). It can be seen that the UOCA of the Pro-CBPM is greater than 150° even in the water environment of pH = 3 and 11, demonstrating that the paper-based materials have good wettability stability in a wide pH range.

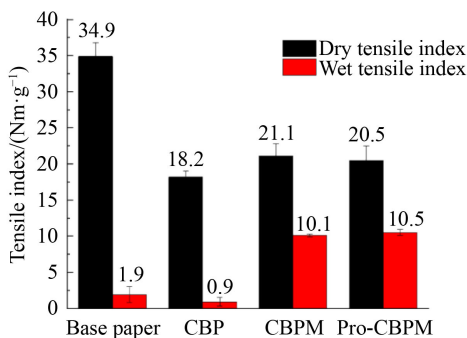


Fig. 2 The tensile indexes of different paper-based materials.

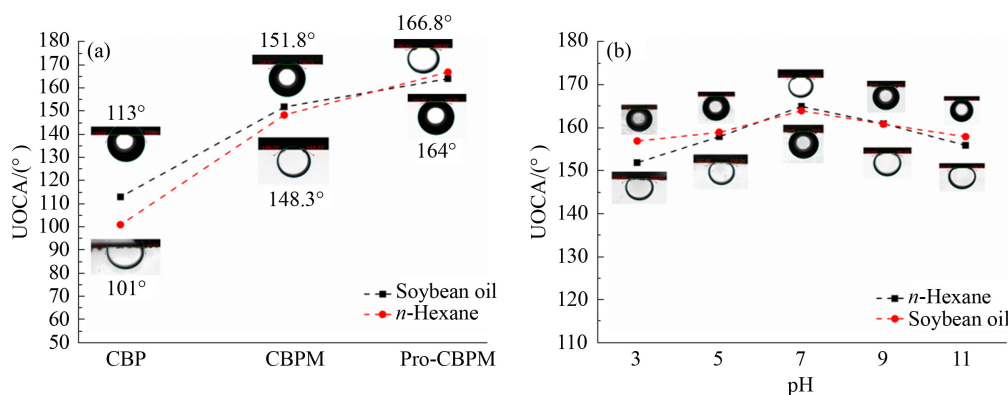


Fig. 3 UOCAs of (a) different paper-based materials for series oils, and (b) the Pro-CBPM in a broad pH range environment.

Table 1 Details and separation performance of paper-based materials

Sample	Maximum pore size/ μm	Porosity/%	Membrane flux/ $(\text{L}\cdot\text{m}^{-2}\cdot\text{h}^{-1})$	Separation efficiency/%
Base paper	26	30.0	274	–
CBP	31	42.0	1207	–
CBPM	30	46.2	1251	–
Pro-CBPM	35	69.8	2020	99.3%

performance of Pro-CBPM, and the results are shown in Fig. 4. The filtrate is almost clear, and there are no observable oil droplets in the microscope photos. The oil/water separation efficiency of the paper-based material reaches 99.3%. In the separation process, the interception of oil droplets can be achieved due to the underwater oleophobicity and smaller pore size of the material surface. However, the small pore size reduce the flux to a great degree. A feasible method is to increase the water flux of the material by increasing the porosity of the material while retaining a high separation efficiency. Overall, the Pro-CBPM possess the advantages in mechanical strength, membrane flux and separation efficiency.

3.5 Adsorption performance of Pro-CBPM

3.5.1 Adsorption kinetics

The pH of the solution is an important influence factor affecting the adsorption process [43]. At lower pH values, the number of active sites that can effectively adsorb heavy metal ions decreases due to protonation of carboxyl groups. Meanwhile, low pH environment enhances the competitive adsorption of hydrogen ions. When the pH is

higher than 6, metal hydroxide precipitates will be formed, leading to errors in experimental results. Therefore, in the follow-up heavy metal adsorption experiments, the optimal pH value is 5. For MB, it has a positive charge in solution. At $\text{pH} < 4$, the adsorption capacity of MB is low due to the fierce competition between H^+ and MB active sites. At $\text{pH} > 4$, due to electrostatic attraction, the adsorption capacity increases and remains stable at pH 6. Therefore, in the following experiment, pH of 6 was selected to study the adsorption of MB.

In general, the adsorption kinetics equation is used to clarify the adsorption process of metal ions and dyes in water. The non-linear forms of pseudo-first-order (4) and pseudo-second-order model (5) can be expressed as follows [44,45]:

$$q_t = q_e (1 - e^{-k_1 t}), \quad (4)$$

$$q_t = \frac{k_2 q_e^2 t}{1 + k_2 q_e t}, \quad (5)$$

where q_e and q_t are the adsorption capacity of adsorbent at equilibrium and time t ($\text{mg} \cdot \text{g}^{-1}$), k_1 (min^{-1}) and k_2 ($\text{g} \cdot \text{mg}^{-1} \cdot \text{min}^{-1}$) are the rate constant. The consistency

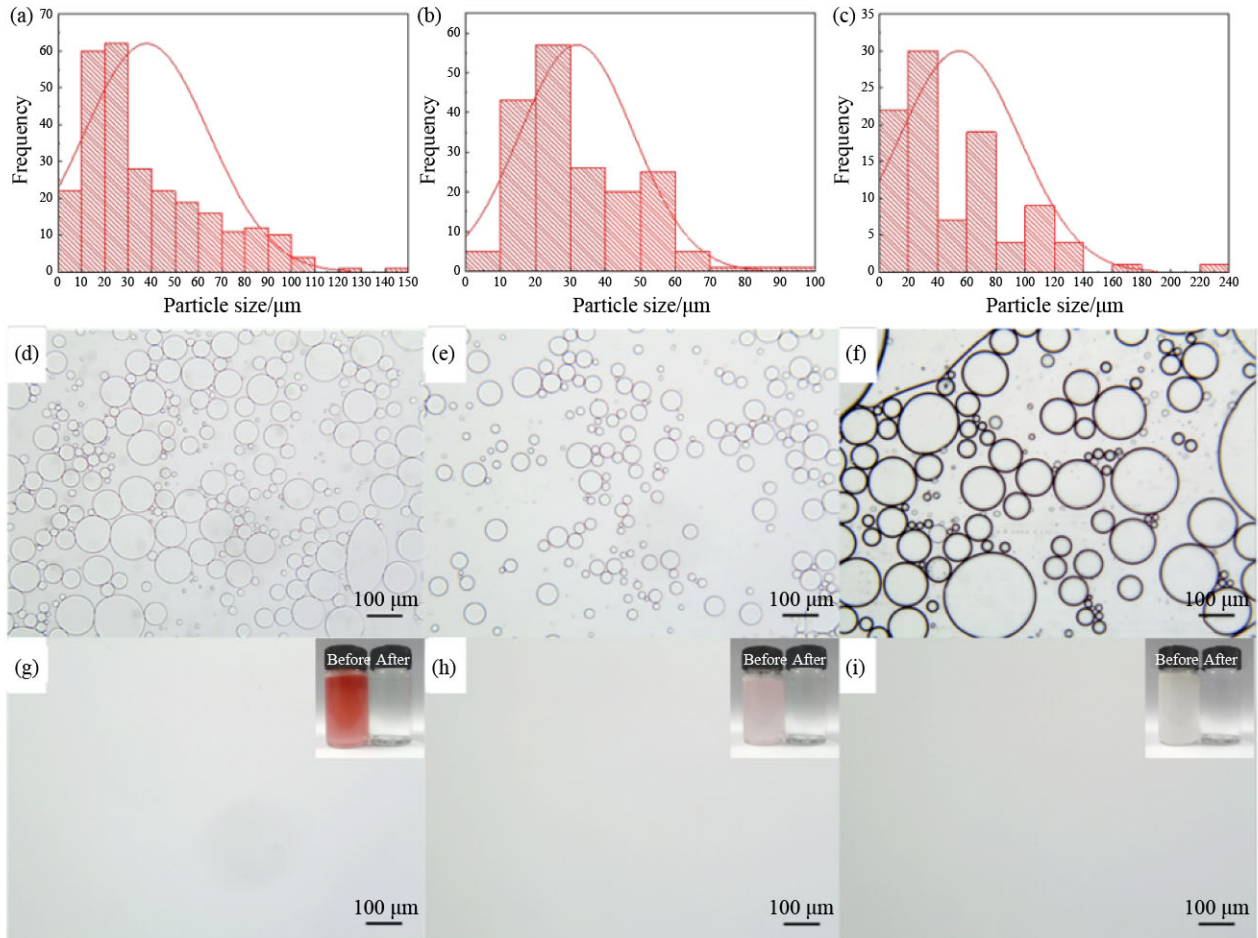


Fig. 4 Particle size distribution and digital pictures of oil–water emulsions before and after filtration separation. (a, d, g) Petroleum ether; (b, e, h) *n*-hexane; (c, f, i) soybean oil petroleum ether.

between actual and predicted values was evaluated by correlation coefficient (R^2).

The adsorption quantities of Pro-CBPM for Cd(II), Pb(II) and MB with time were recorded, and the fitting results are presented in Fig. 5 and Table 2. It can be seen that the pseudo-second-order model has better fitting effect with higher R^2 value. The pseudo-second-order reaction describes the chemisorption process in which adsorbents and adsorbates bind by electron sharing or exchange [46], and the functional groups and specific surface area of the adsorbent play an important role. The reaction between CA and cellulose introduces a large amount of carboxyl groups, which provide more active sites for adsorption. Meanwhile, the high porosity and micropores of straw pulp fiber are also conducive to the internal diffusion of adsorbate. The adsorption mechanism of metal ions mainly relies on the chemical process of forming ionic bonds by the chelation of carboxyl groups and metal cations. The hydrogen bonding and electrostatic attraction between paper adsorbent and MB molecules are the main reasons for MB adsorption.

3.5.2 Adsorption isotherm

In order to describe the equilibrium relationship of adsorbents at the interface of two phases at a certain temperature, the Langmuir and Freundlich models were used for adsorption isotherm analysis. The non-linear equations of Langmuir (6) and Freundlich (7) isotherms are as follows [44,47]:

$$Q_e = \frac{Q_m k_1 C_e}{1 + k_1 C_e} \quad (6)$$

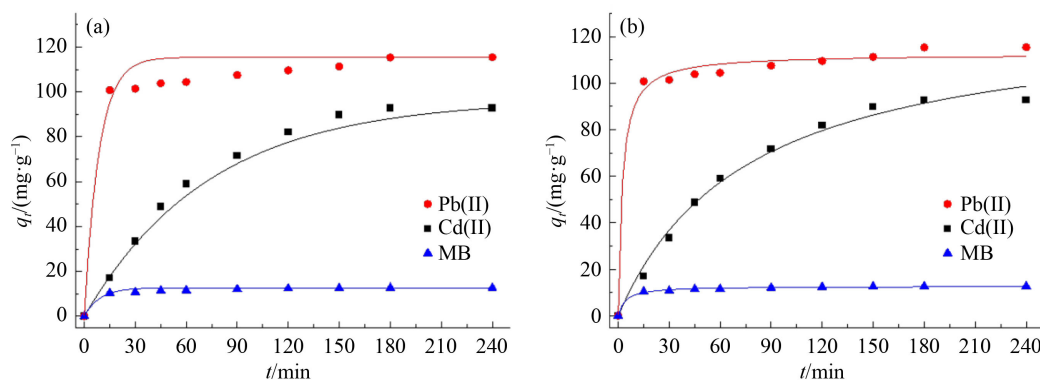


Fig. 5 Kinetic fitting for the adsorption of Cd(II), Pb(II) and MB: (a) Pseudo-first-order kinetics; (b) pseudo-second-order kinetics.

Table 2 Kinetic parameters for Pro-CBPM of Cd(II), Pb(II) and MB

Molecule	$q_{e,e}/(\text{mg}\cdot\text{g}^{-1})$	Pseudo-first-order kinetics			Pseudo-second-order kinetics		
		$q_{e,c}$	k_1	R^2	$q_{e,c}$	k_2	R^2
Cd(II)	92.8	96.6	0.013	0.984	129.9	0.0001	0.900
Pb(II)	115.4	115.5	0.116	0.948	112.6	0.0037	0.992
MB	12.7	12.7	0.109	0.956	12.7	0.0190	0.994

$$Q_e = k_f C_e^{\frac{1}{n}} \quad (7)$$

where C_e ($\text{mg}\cdot\text{L}^{-1}$) is the concentration at the equilibrium, Q_e and Q_m are the equilibrium and maximum adsorption capacity ($\text{mg}\cdot\text{g}^{-1}$), k_1 ($\text{L}\cdot\text{mg}^{-1}$), k_f and n are isothermal constant, the constant related to the adsorption capacity and strength, respectively.

Figure 6 and Table 3 show the fitted results for the adsorption isotherm data. According to R^2 , the Langmuir isotherm model fits the adsorption process of heavy metal ions and MB better, indicating that the adsorption is mainly monolayer adsorption [48]. According to the Langmuir model, the theoretical maximum adsorption capacities of Pro-CBPM for Cd(II), Pb(II) and MB were 136, 229 and $128.9 \text{ mg}\cdot\text{g}^{-1}$, respectively. Paper-based material, which has the integrated performance in heavy metal ion adsorption, dye adsorption, oil–water separation, solves the drawback of single processing capacity for traditional water-treatment materials.

3.6 Practical application of Pro-CBPM in the complex wastewater

The prepared multifunctional paper-based material has good oil–water emulsion separation ability as well as heavy metal ion and dye adsorption capacities. In practice, pollutants in wastewater are often complex and mixed. The multifunctional membrane can be combined with the circulating filtration device to realize the simultaneous treatment of various pollutants. A practical treatment process of simulated complex wastewater is designed using the paper-based materials, as shown in Scheme 2. When the wastewater containing emulsified oil passes through Pro-CBPM, the water is easy to pass

through and the oil droplets are intercepted because of the underwater superoleophobicity. At the same time, the abundant carboxyl groups of paper-based materials can effectively remove metal ions and dyes in cycling adsorption, greatly shortening the adsorption time. In addition, owing to the paper morphology and high robustness, it can be easily installed and recycled. The practical application performance of the paper-based material in the cycling experiment was also evaluated. During the cyclic oil–water separation, deionized water was used to wash off the attached oil after each time. After 5 cycles of adsorption and desorption, the oil–water separation efficiency and adsorption capacity retained above 98.5% and 80%, respectively.

4 Conclusions

Based on the idea of high-value utilization of high-yield grass pulp, the paper-based adsorption–separation

material with low cost, high porosity and high wet strength was prepared by green papermaking process with CA as crosslinking agent and modifier and CC as pore-forming agent. The porosity of Pro-CBPM was increased to 69.8% by pore formation, which was greatly higher than that of base paper. The reaction of CA with fiber increased the wet strength and introduced a large number of adsorption sites with the carboxyl content of $0.91 \text{ mmol}\cdot\text{g}^{-1}$. Combined with the high specific surface area of the material, the theoretical maximum adsorption capacity of Pro-CBPM for Cd(II), Pb(II) and MB were up to 136, 229 and $128 \text{ mg}\cdot\text{g}^{-1}$, respectively. Due to the construction of a hierarchical micro-nano structure, the paper also has good oil–water separation performance. The UOCA of Pro-CBPM was high up to 165° , and the separation efficiency of emulsified oil reached 99.3%. The paper-based material, which integrates oil/water separation, dye adsorption, and heavy metal ion adsorption, has important application value in complex wastewater treatment.

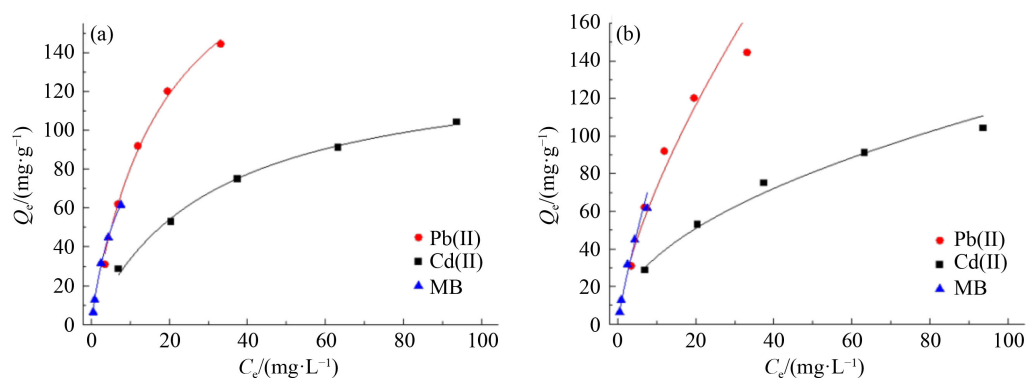
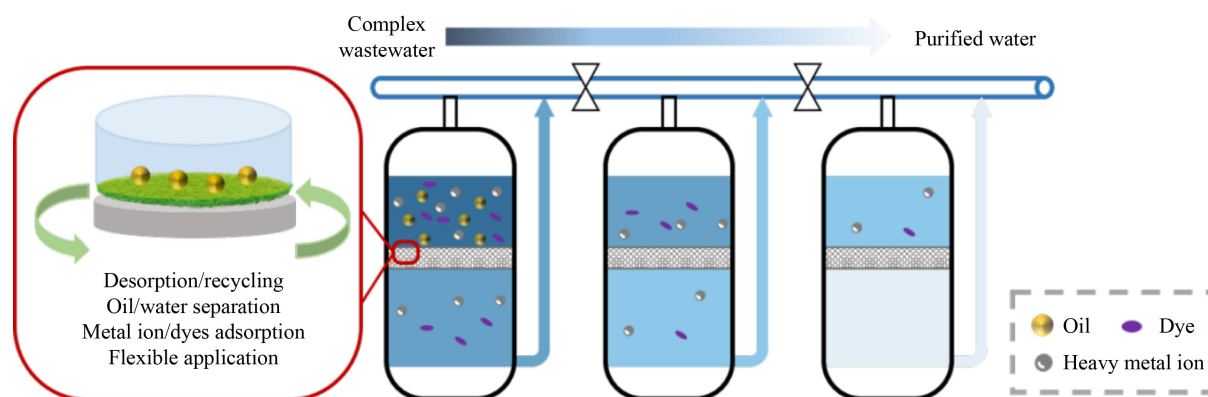


Fig. 6 Isotherms fitting for the adsorption of Cd(II), Pb(II) and MB: (a) Langmuir isotherm; (b) Freundlich isotherm.

Table 3 Isotherms parameters for Pro-CBPM of Cd(II), Pb(II) and MB

Molecule	Langmuir isotherm			Freundlich isotherm		
	$Q_m/(\text{mg}\cdot\text{g}^{-1})$	$k_f/(\text{L}\cdot\text{mg}^{-1})$	R^2	n	k_f	R^2
Cd(II)	136.8	0.032	0.994	1.98	11.17	0.972
Pb(II)	229.0	0.053	0.992	1.46	15.00	0.903
MB	128.9	0.121	0.997	1.15	12.09	0.938



Scheme 2 Schematic of adsorption and separation technological process using multi-functional paper-based material.

Acknowledgements The support of this work by the National Key Research and Development Program of China (Grant No. 2019YFC19059003) and the Priority Academic Program Development of Jiangsu Higher Education Institutions (PAPD) is gratefully acknowledged.

Electronic Supplementary Material Supplementary material is available in the online version of this article at <https://dx.doi.org/10.1007/s11705-022-2267-7> and is accessible for authorized users.

References

- Zhao W, Chen I, Huang F. Toward large-scale water treatment using nanomaterials. *Nano Today*, 2019, 27: 11–27
- Ali I, Gupta V K. Advances in water treatment by adsorption technology. *Nature Protocols*, 2006, 1(6): 2661–2667
- Fu F, Wang Q. Removal of heavy metal ions from wastewaters: a review. *Journal of Environmental Management*, 2011, 92(3): 407–418
- Li G, Mai Z, Shu X, Chen D, Liu M, Xu W. Superhydrophobic/superoleophilic cotton fabrics treated with hybrid coatings for oil/water separation. *Advanced Composites and Hybrid Materials*, 2019, 2(2): 254–265
- Thai A N, Juang R S. Treatment of waters and wastewaters containing sulfur dyes: a review. *Chemical Engineering Journal*, 2013, 219: 109–117
- Gu J, Xiao P, Chen P, Zhang L, Wang H, Dai L, Song L, Huang Y, Zhang J, Chen T. Functionalization of biodegradable PLA nonwoven fabric as superoleophilic and superhydrophobic material for efficient oil absorption and oil/water separation. *ACS Applied Materials & Interfaces*, 2017, 9(7): 5968–5973
- Wu M, Shi G, Liu W, Long Y, Mu P, Li J. A universal strategy for the preparation of dual superlyophobic surfaces in oil–water systems. *ACS Applied Materials & Interfaces*, 2021, 13(12): 14759–14767
- Zare E N, Motahari A, Sillanpaa M. Nanoadsorbents based on conducting polymer nanocomposites with main focus on polyaniline and its derivatives for removal of heavy metal ions/dyes: a review. *Environmental Research*, 2018, 162: 173–195
- Huang D, Chen N, Dai W, Zheng M, Wang M, Qian Y, Xu P. Preparation and adsorption properties of aminated magnetic carbon nanotubes. *Journal of Forestry Engineering*, 2022, 7: 100–106
- Abdel-Hakim A, Abdella A H, Sabaa M W, Gohar H Y, Mohamed R R, Tera F M. Performance evaluation of modified fabricated cotton membrane for oil/water separation and heavy metal ions removal. *Journal of Vinyl and Additive Technology*, 2021, 27(4): 933–945
- Zhong Q, Shi G, Sun Q, Mu P, Li J. Robust PVA-GO-TiO₂ composite membrane for efficient separation oil-in-water emulsions with stable high flux. *Journal of Membrane Science*, 2021, 640: 119836
- Ao C, Hu R, Zhao J, Zhang X, Li Q, Xia T, Zhang W, Lu C. Reusable, salt-tolerant and superhydrophilic cellulose hydrogel-coated mesh for efficient gravity-driven oil/water separation. *Chemical Engineering Journal*, 2018, 338: 271–277
- Wang Z, Ji S, Zhang J, Liu Q, Fang H, Peng S, Li Y. Tannic acid encountering ovalbumin: a green and mild strategy for superhydrophilic and underwater superoleophobic modification of various hydrophobic membranes for oil/water separation. *Journal of Materials Chemistry A: Materials for Energy and Sustainability*, 2018, 6(28): 13959–13967
- Chen J, Zhou Y, Zhou C, Wen X, Xu S, Cheng J, Pi P. A durable underwater superoleophobic and underoil superhydrophobic fabric for versatile oil/water separation. *Chemical Engineering Journal*, 2019, 370: 1218–1227
- Cao H, Liu Y. Facile design of a stable and inorganic underwater superoleophobic copper mesh modified by self-assembly sodium silicate and aluminum oxide for oil/water separation with high flux. *Journal of Colloid and Interface Science*, 2021, 598: 483–491
- Li J, Zuo K, Wu W, Xu Z, Yi Y, Jing Y, Dai H, Fang G. Shape memory aerogels from nanocellulose and polyethyleneimine as a novel adsorbent for removal of Cu(II) and Pb(II). *Carbohydrate Polymers*, 2018, 196: 376–384
- Zhang X, Tian J, Wang P, Liu T, Ahmad M, Zhang T, Guo J, Xiao H, Song J. Highly-efficient nitrogen self-doped biochar for versatile dyes' removal prepared from soybean cake via a simple dual-templating approach and associated thermodynamics. *Journal of Cleaner Production*, 2022, 332: 130069
- Ma J, Wang X, Fu Q, Si Y, Yu J, Ding B. Highly carbonylated cellulose nanofibrous membranes utilizing maleic anhydride grafting for efficient lysozyme adsorption. *ACS Applied Materials & Interfaces*, 2015, 7(28): 15658–15666
- Liu Q, Li Y, Chen H, Lu J, Yu G, Moslang M, Zhou Y. Superior adsorption capacity of functionalised straw adsorbent for dyes and heavy-metal ions. *Journal of Hazardous Materials*, 2020, 382: 121040
- Chen Y, Chen L, Bai H, Li L. Graphene oxide-chitosan composite hydrogels as broad-spectrum adsorbents for water purification. *Journal of Materials Chemistry A: Materials for Energy and Sustainability*, 2013, 1(6): 1992–2001
- Ma L, Dong X, Chen M, Zhu L, Wang C, Yang F, Dong Y. Fabrication and water treatment application of carbon nanotubes (CNTs)-based composite membranes: a review. *Membranes*, 2017, 7(1): 16
- Peng B, Yao Z, Wang X, Crombeen M, Gsweeney D G, Tam K C. Cellulose-based materials in wastewater treatment of petroleum industry. *Green Energy & Environment*, 2020, 5(1): 37–49
- Hong C. Recent progress in using hybrid silicon polymer composites for wastewater treatment. *Chemosphere*, 2020, 263: 128380
- Li D, Li Q, Mao D, Bai N, Dong H. A versatile bio-based material for efficiently removing toxic dyes, heavy metal ions and emulsified oil droplets from water simultaneously. *Bioresource Technology*, 2017, 245: 649–655
- Malhotra P, Jain A. Graphene oxide-based nanocomposites for adsorptive removal of water pollutants. *Contamination of Water*, 2021: 431–448
- Jiang S, Xi J, Dai H, Wu W, Xiao H. Multifunctional cellulose paper-based materials and their application in complex

- wastewater treatment. *International Journal of Biological Macromolecules*, 2022, 207: 414–423
27. Miao X, Lin J, Bian F. Utilization of discarded crop straw to produce cellulose nanofibrils and their assemblies. *Journal of Bioresources and Bioproducts*, 2020, 5(1): 26–36
 28. Cai T, Li H, Yang R, Wang Y, Li R, Yang H, Li A, Cheng R. Efficient flocculation of an anionic dye from aqueous solutions using a cellulose-based flocculant. *Cellulose*, 2015, 22(2): 1439–1449
 29. Jin H, Capareda S, Chang Z, Gao J, Xu Y, Zhang J. Biochar pyrolytically produced from municipal solid wastes for aqueous As(V) removal: adsorption property and its improvement with KOH activation. *Bioresource Technology*, 2014, 169: 622–629
 30. Ayoub A, Venditti R A, Pawlak J J, Salam A, Hubbe M A. Novel hemicellulose-chitosan biosorbent for water desalination and heavy metal removal. *ACS Sustainable Chemistry & Engineering*, 2013, 1(9): 1102–1109
 31. Chen Y, Wang Y, Wan J, Ma Y. Crystal and pore structure of wheat straw cellulose fiber during recycling. *Cellulose*, 2010, 17(2): 329–338
 32. Jiang S, Xi J, Deng W, Dai H, Fang G, Wu W. Low-cost and high-wet-strength paper-based lignocellulosic adsorbents for the removal of heavy metal ions. *Industrial Crops and Products*, 2020, 158: 112926
 33. Wang Z, Jiang X, Cheng X, Lau C H, Shao L. Mussel-inspired hybrid coatings that transform membrane hydrophobicity into high hydrophilicity and underwater superoleophobicity for oil-in-water emulsion separation. *ACS Applied Materials & Interfaces*, 2015, 7(18): 9534–9545
 34. Hoeng F, Denneulin A, Neuman C, Bras J. Charge density modification of carboxylated cellulose nanocrystals for stable silver nanoparticles suspension preparation. *Journal of Nanoparticle Research*, 2015, 17(6): 1–14
 35. Zhou J, Butchosa N, Jayawardena H S N, Park J, Zhou Q, Yan M, Ramstrom O. Synthesis of multifunctional cellulose nanocrystals for lectin recognition and bacterial imaging. *Biomacromolecules*, 2015, 16(4): 1426–1432
 36. Wang B, Liang W, Guo Z, Liu W. Biomimetic super-lyophobic and super-lyophilic materials applied for oil/water separation: a new strategy beyond nature. *Chemical Society Reviews*, 2015, 44(1): 336–361
 37. Tang L, Li T, Zhuang S, Lu Q, Li P, Huang B. Synthesis of pH-sensitive fluorescein grafted cellulose nanocrystals with an amino acid spacer. *ACS Sustainable Chemistry & Engineering*, 2016, 4(9): 4842–4849
 38. Rajala H. The effect of size and structure of filler particles on paper properties. Thesis for the Bachelor's Degree. Tampere: Tampere University of Applied Science, 2012
 39. Jung S, Tiwari M K, Doan N V, Poulidakos D. Mechanism of supercooled droplet freezing on surfaces. *Nature Communications*, 2012, 3(1): 1–8
 40. Chen X, Chen D, Li N, Xu Q, Li H, He J, Lu J. Modified-MOF-808-loaded polyacrylonitrile membrane for highly efficient, simultaneous emulsion separation and heavy metal ion removal. *ACS Applied Materials & Interfaces*, 2020, 12(35): 39227–39235
 41. Wei D W, Wei H, Gauthier A C, Song J, Xiao H. Superhydrophobic modification of cellulose and cotton textiles: methodologies and applications. *Journal of Bioresources and Bioproducts*, 2020, 5(1): 1–15
 42. Qu M, He D, Luo Z, Wang R, Shi F, Pang Y, Sun W, Peng L, He J. Facile preparation of a multifunctional superhydrophilic pvdf membrane for highly efficient organic dyes and heavy metal ions adsorption and oil/water emulsions separation. *Colloids and Surfaces A: Physicochemical and Engineering Aspects*, 2022, 637: 128231
 43. Yu P, Wang X, Zhang K, Wu M, Wu Q, Liu J, Yang J, Zhang J. Continuous purification of simulated wastewater based on rice straw composites for oil/water separation and removal of heavy metal ions. *Cellulose*, 2020, 27(9): 5223–5239
 44. Febrianto J, Kosasih A N, Sunarso J, Ju Y, Indraswati N, Ismadji S. Equilibrium and kinetic studies in adsorption of heavy metals using biosorbent: a summary of recent studies. *Journal of Hazardous Materials*, 2009, 162(2-3): 616–645
 45. Ho Y S, Mckay G. Pseudo-second order model for sorption processes. *Process Biochemistry*, 1999, 34(5): 451–465
 46. Vazquez G, Calvo M, Sonia Freire M, Gonzalez-Alvarez J, Antorrena G. Chestnut shell as heavy metal adsorbent: optimization study of lead, copper and zinc cations removal. *Journal of Hazardous Materials*, 2009, 172(2-3): 1402–1414
 47. Wang L, Zhao X, Zhang J, Xiong Z. Selective adsorption of Pb(II) over the zinc-based MOFs in aqueous solution-kinetics, isotherms, and the ion exchange mechanism. *Environmental Science and Pollution Research International*, 2017, 24(16): 14198–14206
 48. Li Y, Zhu H, Zhang C, Cheng M, He H. Pei-grafted magnetic cellulose for Cr(VI) removal from aqueous solution. *Cellulose*, 2018, 25(8): 4757–4769